



FATIGUE DESIGN 2021, 9th Edition of the International Conference on Fatigue Design

## Fatigue design of mild and high-strength steel cruciform joints in as-welded and HFMI-treated condition by nominal and effective notch stress approach

Peter Brunnhofer\*, Christian Buzzi, Tobias Pertoll, Martin Rieger, Martin Leitner

*Graz University of Technology, Institute of Structural Durability and Railway Technology, Inffeldgasse 25/D, 8010 Graz, Austria*

---

### Abstract

According to the Recommendations for Fatigue Design of Welded Joints and Components by the International Institute of Welding (IIW), the fatigue strength of welded steel joints is in general independent of the base material strength. Post-treatment methods, such as the High Frequency Mechanical Impact (HFMI) treatment, can significantly increase the fatigue performance of welded joints especially in case of high-strength steel applications, which is already considered within the IIW Recommendations for the HFMI Treatment. This paper firstly investigates the effect of the base material strength on the fatigue resistance of welded and HFMI-treated steel joints. Therefore, mild steel S355 and high-strength steel S700 cruciform joints are cyclically tested in both conditions and the statistically evaluated S/N-curves are compared. The results reveal an increase of the high-cycle fatigue strength by the HFMI-treatment by a factor of 1.35 in case of the S355, and of 1.59 for the S700 specimens. Secondly, the test results are assessed by the fatigue design curves of the corresponding structural detail within the IIW-recommendations using the nominal stress concept. Moreover, the applicability of the procedure applying the effective notch approach is analyzed. In order to numerically evaluate the effective notch stress, the geometry of the cruciform joint is modelled according to the given guidelines within the recommendations applying a reference radius of 1 mm at the weld toe for both conditions. On the basis of the numerically computed effective notch stress, a local fatigue design is performed for all test series, which reveals sound accordance between the recommended design curves and the statistically evaluated fatigue test S/N-curves.

© 2021 The Authors. Published by Elsevier B.V.

This is an open access article under the CC BY-NC-ND license (<https://creativecommons.org/licenses/by-nc-nd/4.0>)

Peer-review under responsibility of the scientific committee of the Fatigue Design 2021 Organizers

**Keywords:** Fatigue design, Welded joints, High-strength steel, HFMI-treatment, Effective notch stress approach.

---

## 1. Introduction

Due to residual stresses (Friedrich, 2020; Nitschke-Pagel and Hensel, 2021; Sonsino, 2009b), local and/or global geometry (Harati et al., 2015; Ottersböck et al., 2018; Ottersböck et al., 2019) and microstructural effects (Trudel et al., 2014; Tsay and Tsay; Yamaguchi et al., 2019) as well as imperfections (Leitner et al., 2018a; Liinalampi et al., 2019; Ottersböck et al., 2021), the fatigue strength of weld joints is considered as independent of the base material strength, compare to the IIW recommendations for fatigue design of welded joints and components by (Hobbacher, 2016). Due to post-treatment techniques, the fatigue strength may be improved, see the IIW Recommendations on methods for improving the fatigue strength of welded joints by (Haagensen and Maddox). Besides common methods, such as burr-grinding (Braun and Wang, 2021; Hansen et al., 2007; Zhang and Maddox, 2009), TIG-dressing (Dahle, 1998; Huo et al., 2005; Mettänen et al., 2020), shot peening (Gan et al., 2016; Hensel et al., 2019; Kinoshita et al., 2019), hammer/needle peening (Fu et al., 2018; Fueki et al., 2019; Tai and Miki, 2014) or post-weld heat treatment (Hirohata, 2017; Leitner et al., 2015; RAVI et al., 2005), the High Frequency Mechanical Impact (HFMI) treatment can lead to a significant increase of the fatigue performance of welded structures (Harati et al., 2016; Leitner et al., 2014; Yildirim and Marquis, 2012a).

As the HFMI-induced local compressive residual state acts as significant fundament for the benefit by the post-treatment method (Leitner, 2017), increased mean stress conditions (Leitner and Stoschka, 2020) or also variable amplitude loads (Leitner et al., 2018b) may affect the stability of the local compressive residual stress state (Leitner et al., 2017a) hence impacting the increase of the fatigue strength. Based on numerous fatigue test data, e.g. summarized in (Yildirim and Marquis, 2012b), IIW recommendations for the HFMI treatment for improving the fatigue strength of welded joints were published by (Marquis and Barsoum, 2016), which are validated by further test data, e.g. given in (Leitner et al., 2020; Leitner and Barsoum, 2020; Yıldırım et al., 2016). To enable a fatigue design of complexly-shaped weld structures, the application of local approaches is favorable (Leitner et al., 2017c; Schubnell et al., 2017; Yildirim et al., 2013), whereas the IIW recommendations for the HFMI treatment provide design values by modelling the HFMI-treated weld toe by a reference radius of  $r_{ref} = 1$  mm, see also (Yildirim and Marquis, 2014), according to the effective notch stress approach as given in (Sonsino, 2009a) and (Hobbacher, 2016).

Hence, this paper scientifically contributes to the fatigue assessment based on both nominal and effective notch stresses. Focus is laid on cruciform joints manufactured with two different steel grades, a mild steel S355 and a high-strength steel S700. Fatigue tests in as-welded and HFMI-treated condition for both base materials proof the beneficial effect by the post-treatment method. Numerical analysis is applied to evaluate the effective notch stress concentration factors as basis for the local fatigue assessment. Finally, the results by the experiments are compared to the design values given in (Hobbacher, 2016) for the as-welded and in (Marquis and Barsoum, 2016) for the HFMI-treated test series for validation purposes. A final outlook provides suggestions to prospective working topics in this field.

### Nomenclature

|                |                                                     |
|----------------|-----------------------------------------------------|
| $A_5$          | elongation at fracture                              |
| $E$            | Youngs's modulus                                    |
| $f_y$          | yield strength                                      |
| $f_u$          | ultimate strength                                   |
| $f(t)$         | thickness reduction factor                          |
| $K_t$          | stress concentration factor                         |
| $m_{1/2}$      | slope of the S/N-curve above / below the knee point |
| $n$            | thickness correction exponent                       |
| $r$            | weld toe radius                                     |
| $R$            | load stress ratio                                   |
| $\sigma$       | stress                                              |
| $\Delta\sigma$ | stress range                                        |
| $t$            | plate thickness                                     |
| $\mu$          | Poisson's ratio                                     |

## 2. Base material and specimen design

The mechanical properties and the chemical compositions of the two sets of specimens made of mild steel S355 and high-strength steel S700 are shown in Table 1 to Table 4.

Table 1: Chemical composition (in weight %) of high-strength steel S700

| C     | Si    | Mn    | P     | S      | Al    | Cr     |
|-------|-------|-------|-------|--------|-------|--------|
| 0.067 | 0.031 | 1.900 | 0.007 | 0.0017 | 0.057 | 0.032  |
| Ni    | Mo    | Cu    | V     | Nb     | Ti    | B      |
| 0.022 | 0.008 | 0.019 | 0.007 | 0.050  | 0.139 | 0.0002 |

Table 2: Mechanical properties of high-strength steel S700

| Yield strength $f_y$ | Ultimate strength $f_u$ | Elongation at fracture $A_5$ | Impact toughness at $-40^\circ\text{C}$ |
|----------------------|-------------------------|------------------------------|-----------------------------------------|
| 772 MPa              | 807 MPa                 | 19.8 %                       | 112 J                                   |

Table 3: Nominal chemical composition (in weight %) of mild steel S355J2W

| C    | Si   | Mn   | P    | S    | Cu   | Cr   | Ni   | Mo   | Zr   |
|------|------|------|------|------|------|------|------|------|------|
| 0.16 | 0.50 | 1.50 | 0.03 | 0.03 | 0.55 | 0.80 | 0.65 | 0.03 | 0.15 |

Table 4: Nominal mechanical properties of mild steel S355J2W

| Yield strength $f_y$ | Ultimate strength $f_u$ | Elongation at fracture $A_5$ | Impact toughness at $-40^\circ\text{C}$ |
|----------------------|-------------------------|------------------------------|-----------------------------------------|
| $\geq 355$ MPa       | (510 ... 680) MPa       | $\geq 22$ %                  | 27 J                                    |

The base plate of the S355 cruciform specimens has a thickness  $t = 12.5$  mm. The dimensions of the welded specimen can be taken from Figure 1. The specimens are manually welded to plates by GMAW using an active shielding gas, with three specimens in each plate.

The base plate of the high-strength steel S700 specimens exhibits a thickness of  $t = 10$  mm. The geometry of the examined load-carrying cruciform from S700 can be seen in Figure 2. The S700 weld assemblies are gas metal arc welded using a robot with M21 shielding gas.

The weld specimens, both the mild steel and high strength steel, are subsequently machined out of the welded plates.

Subsequent to the welding process, from both series about half of the specimens are HFMI-treated at the four weld toes using the PIT system. High frequency mechanical impact (HFMI) treatment was performed with the frequency of 90 Hz and using indenters with radii of 2 mm.

As shown in Leitner et al., 2015 in case of the investigated mild steel S355 joints, the HFMI-treatment significantly improves the weld toe radius from about 0.1 to 1 mm up to a value of about 2 mm equaling the pin radius of the used indenter. Furthermore, a distinctive change in the local residual stress condition is observed due to the post-treatment. Applying the HFMI-treatment, the local residual stress state majorly reduces down to about  $-250$  to  $-350$  MPa at the weld toe surface leading to compressive residual states beneficially contributing to the fatigue strength increase.

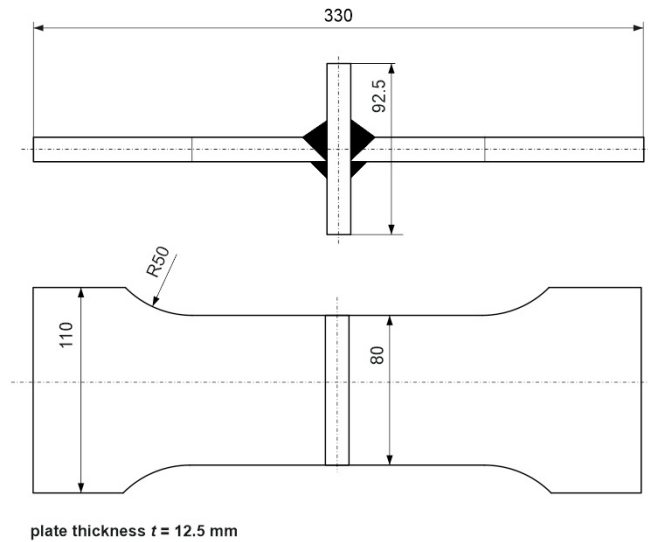


Figure 1: Geometry of the investigated S355 specimen

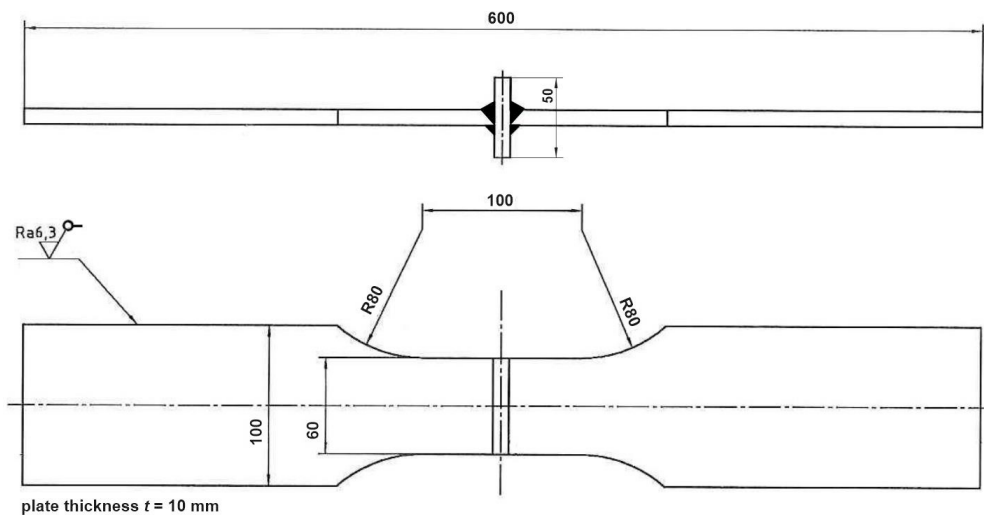


Figure 2: Geometry of the investigated S700 specimen

### 3. Fatigue tests

The fatigue tests were performed under load-controlled uniaxial constant amplitudes loading (CAL) at a load stress ratio of  $R = 0.1$ . The tests with the S355 specimens were conducted on a resonance testing machine, as well as on a servo-hydraulic testing machine for the S700 specimens. The fatigue tests on both testing machines were performed until macro crack initiation or without failure until a defined run-out limit of twenty million load-cycles for the S355 cruciform joints and ten million load-cycles for the S700 specimens respectively.

The crack initiation occurred solely at the weld toe - a typical fracture pattern is shown in Figure 3.



Figure 3: Typical failure mode with crack initiation at the weld toe

### 3.1. Test results

The test results are evaluated according to IIW recommendation (Hobbacher, 2016) for a survival probability of 97.7%. The following applies to the evaluation of S355 and S700 test results. Exponent  $m_1$  for the S/N-curve before the knee point is evaluated based on the test results as well as the position of the knee point. According to (Hobbacher, 2016), the slope after the knee point is set to  $m_2 = 22$ .

The nominal S/N-curve for the as-welded and HFMI-treated condition of the mild steel S355 are given in Figure 4. The results reveal that in the finite life region up to a number of about one million load-cycles, no distinctive difference between the test series occurs. However, focusing on the high-cycle fatigue regime, an increase in fatigue strength due to the HFMI-treatment is clearly observable, whereas a benefit factor of 1.35 at two million load-cycles is evaluated, see Table 5.

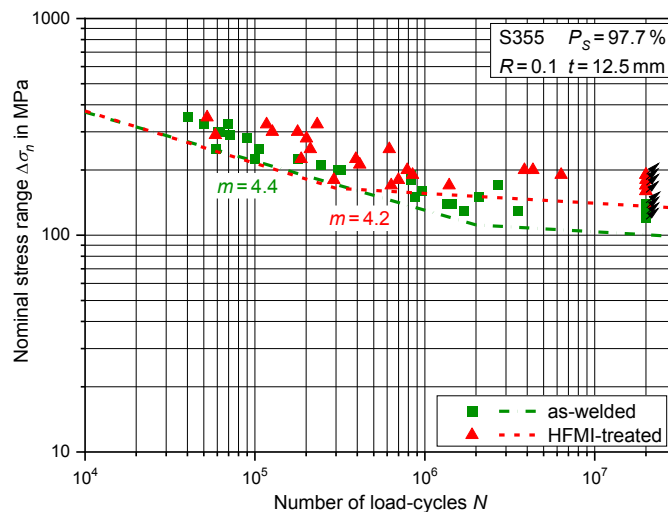


Figure 4 Fatigue test results and S/N-curves of S355 in as-welded and HFMI-treated condition

The test results of the high-strength steel S700 fatigue tests are shown in Figure 5. In this case, in both, finite life and high-cycle fatigue region the post-treatment leads to a fatigue strength enhancement. Again, focusing on two million load-cycles, a benefit factor of 1.59 results from the fatigue test data, see Table 5.

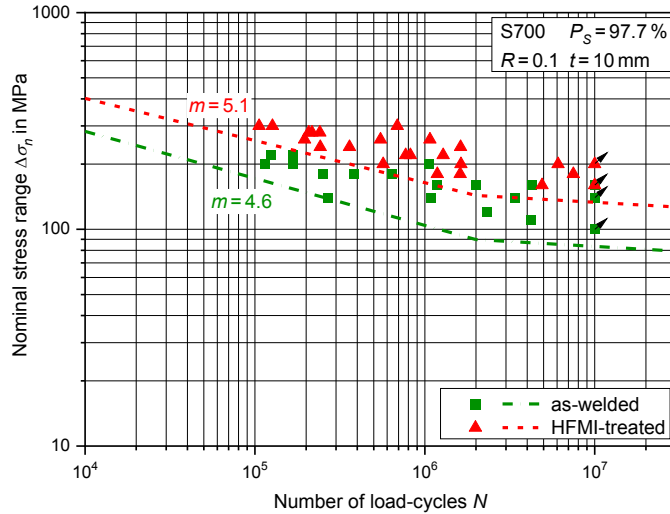


Figure 5 Fatigue test results and S/N-curves of S700 in as-welded and HFMI-treated condition

A summary of the statistically evaluated fatigue test points and the HFMI-benefit factors are provided in Table 5.

Table 5: Benefit of HFMI-treatment

|      | As-welded<br>$\Delta\sigma_{2e6,97.7\%}$ in MPa | HFMI-treated<br>$\Delta\sigma_{2e6,97.7\%}$ in MPa | Benefit factor of HFMI-treatment<br>$\Delta\sigma_{S700,2e6,97.7\%} / \Delta\sigma_{S355,2e6,97.7\%}$ |
|------|-------------------------------------------------|----------------------------------------------------|-------------------------------------------------------------------------------------------------------|
| S355 | 111                                             | 150                                                | 1.35                                                                                                  |
| S700 | 90                                              | 143                                                | 1.59                                                                                                  |

#### 4. Numerical analysis

Aim of the numerical analyses is to calculate notch stress concentration factors  $K_t$  for the as-welded and HFMI-treated S700 specimen. No misalignments such as axial, angular and torsional are considered. In chapter 5.2 the results of the nominal stress fatigue tests are multiplied with  $K_t$  and will be contrasted with the IIW recommendations.

The geometry of the finite element model (FE model) bases on a digital measurement on selected specimen. Using 8-node quadrilateral elements (Baumgartner and Bruder, 2013; Leitner et al., 2017b), it is prepared for a 2D plane strain solution with a linear-elastic behavior. The nominal tension stress is defined with  $\sigma_n = 1$  MPa. For the evaluation, the maximum principal stress is used. Geometry measurements and the simulation is made with the CAE Software Siemens NX Version 1980. The material for the finite element simulation is defined as steel with a Young’s modulus of  $E = 206\,940$  MPa and a Poisson’s ratio  $\mu = 0.288$ , both values are from the material data base of the CAE Software.

##### 4.1. Geometry measurements

The measuring of the geometry for the cruciform joint was performed with the CAE Software. Using pictures of the shape of the cross section taken during the fatigue test. Due to the non-perspective distortion of the telecentric lenses all photos have a fixed scale. Importing three pictures of as-welded and HFMI-treated specimen each into the CAE Software allows to measure angles and distances and transform it to a true to scale model. For the geometric quantities, such as throat depth and flank angle, the mean value of the geometric measurements is used to further generate the FE model for the cruciform joint subsequently, see Figure 6. The notch root radius is defined with the reference radius  $r_{ref} = 1$  mm in all investigated cases.

Table 6 Arithmetic mean values of the S700 specimen used for the finite element model

|                           | Throat depth in mm | Flank angle in ° |
|---------------------------|--------------------|------------------|
| Upper (left) HV-weld seam | 4.65               | 38.79            |
| Lower (left) HV-weld seam | 4.65               | 39.17            |
| Upper (right) fillet weld | 4.82               | 22.56            |
| Lower (right) fillet weld | 4.74               | 22.12            |

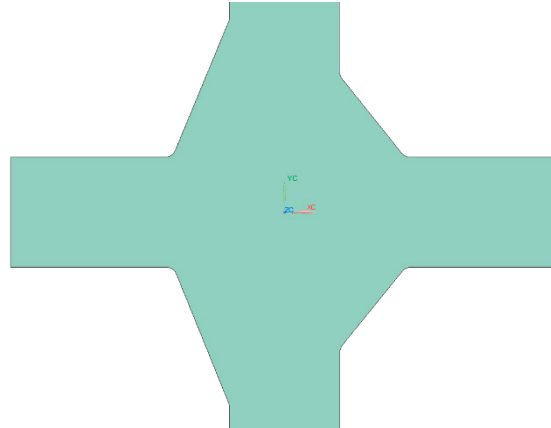


Figure 6 CAD model of a S700 cruciform joint

#### 4.2. Finite Element Model

In order to obtain a practical mesh for the stress analysis, the cross section is divided into two areas. One area is defined with an offset curve of 2 mm using the outer contour of the cruciform joint. It allows the use of a mapped mesh with an element edge length of 0.1 mm (Figure 7). The remaining area is meshed with quadrilateral elements with an edge length of 0.1 mm to about 3.5 mm (Figure 8).

Two rigid-body-elements (RBE) are created at both ends of the model for the force application of the tensile load. The reference nodes of the RBE's are used as load application points for the boundary conditions. One reference node of the RBE is used as a force application node. It has a free displacement in longitudinal direction, all other displacements are locked. The second reference node is locked in all translational and rotational displacements.

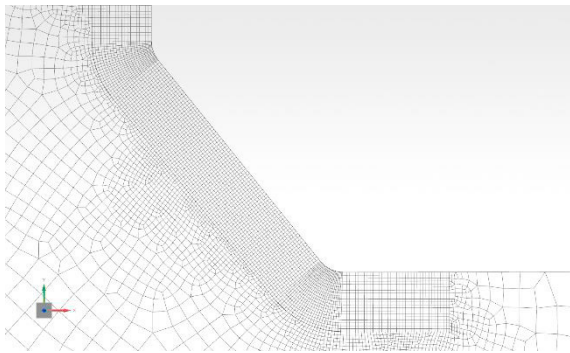


Figure 7 Detail of finite element mesh at the weld seam area

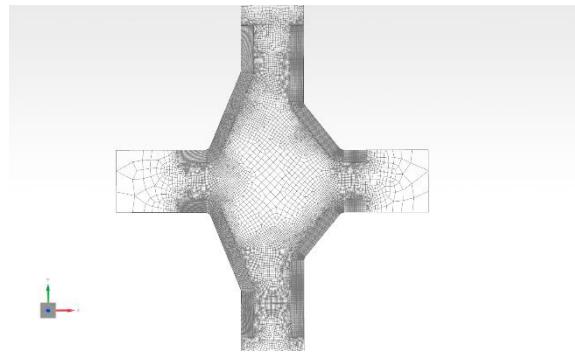


Figure 8 Finite element mesh of the investigated cruciform joints

### 4.3. Numerical results

Performing the simulation and using the maximum principal stress for evaluation it results in a maximum stress concentration factor  $K_t = 2.74$  for the high-strength steel S700 specimens. This is in a similar order of magnitude of  $K_t = 2.76$ , evaluated in (Leitner et al., 2015) for the mild steel S355 specimens.

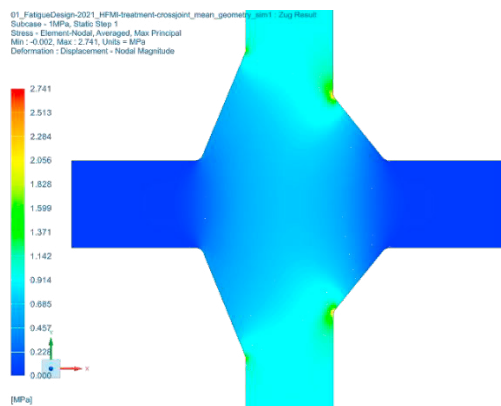


Figure 9 Maximum principal stress distribution

## 5. Fatigue design

### 5.1. Nominal stress approach

Figure 10 and Figure 11 are showing the nominal stress test results of the S355 (Leitner et al., 2015) and S700 cruciform joints for the as-welded and the HFMI-treated state in comparison with the recommended design values (Hobbacher, 2016; Marquis and Barsoum, 2016). As per IIW recommendations (Hobbacher, 2016) the cruciform joint conform to structural detail 413 with a FAT-class of 63 for steel. The fatigue strength can be improved by considering the plate thickness as proposed in (Hobbacher, 2016), using equation (1) with a reference thickness of  $t_{ref} = 25$  mm and an effective thickness  $t_{eff} = 12.5$  mm and  $t_{eff} = 10$  mm respectively. In addition, a thickness correction exponent of  $n = 0.3$  is defined for the as-welded state and  $n = 0.2$  for the HFMI-treated state.

This results in thickness correction factors for the S355 and S700 cruciform joints, both as-welded state, of  $f(t) = 1.23$  and  $f(t) = 1.32$ . The FAT-class can be improved to 78 and 83 respectively. The HFMI-treated cruciform joints are related to the same structural detail as the as-welded specimen. With the proposed improvement for HFMI-treated welds ((Marquis and Barsoum, 2016)) the fatigue resistance for S355 is increased by five classes from FAT 63 to FAT 112. Similarly, the fatigue resistance for S700 is increased by six classes to FAT 125. Applying the plate thickness correction factor  $f(t)$  will lead to FAT 129 and FAT 150 respectively. A summary of the input data for calculating  $f(t)$  and the results are listed in Table 7.

$$f(t) = \left( \frac{t_{ref}}{t_{eff}} \right)^n \tag{1}$$

Table 7 Calculation of thickness correction factor  $f(t)$

| Base material | Condition    | $t_{ref}$ in mm | $t_{eff}$ in mm | $n$ | $f(t)$ |
|---------------|--------------|-----------------|-----------------|-----|--------|
| S355          | As-welded    | 25              | 12.5            | 0.3 | 1.23   |
|               | HFMI-treated | 25              | 12.5            | 0.2 | 1.15   |
| S700          | As-welded    | 25              | 10              | 0.3 | 1.32   |
|               | HFMI-treated | 25              | 10              | 0.2 | 1.20   |

As shown in Figure 10, the statistically evaluated S/N-curve for S355 in as-welded condition has a higher fatigue resistance and flatten slope than the recommendation. Although both curves intersect in the range about 55.000 load-cycles, the bulk of the test data points is still conservatively evaluated applying the IIW recommendation.

Focusing on the HFMI-treated condition, sound agreement is observed in the finite life region. However, in case of higher load-cycles, the recommended S/N-curve leads to a conservative design.

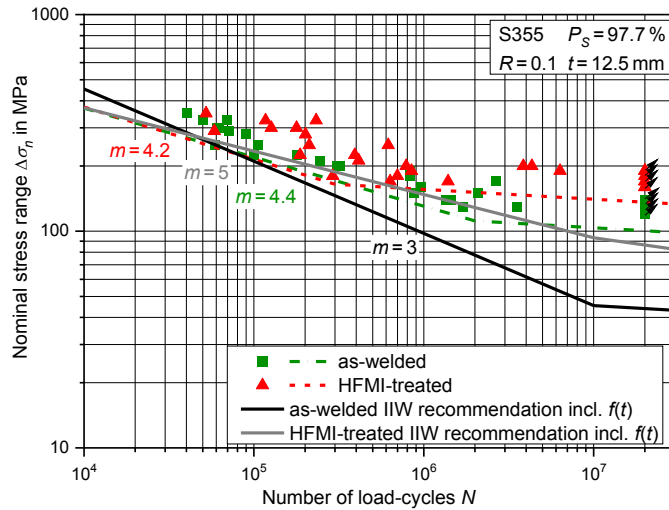


Figure 10: Comparison of test results and IIW recommendation at S355

The results for S700 as-welded condition are shown in Figure 11. The difference between the slopes of  $m_1 = 3$  and  $m_1 = 4.6$  in conjunction with the small gap of the FAT-class results in an overestimation of the test results at lower load-cycles applying the IIW recommendation. This interference is mainly caused by the early failure of one specimen at about 270.000 load-cycles and a nominal stress range  $\Delta\sigma_n = 140$  MPa, which may be caused by a comparably increased specimen deformation. Anyway, again the bulk of the fatigue test data points in the as-welded state is still assessed conservatively based on the design curve. Focusing on the HFMI-treated state, the design curve agrees well to the S/N-curve by tests, revealing a sound applicability of the IIW recommendations for the HFMI treatment.

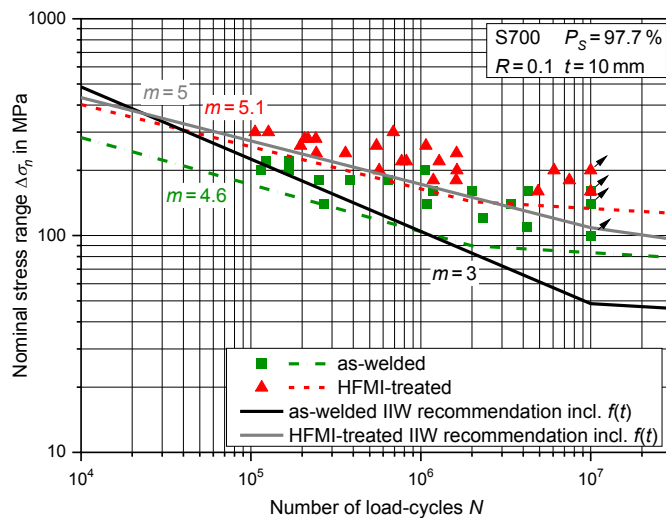


Figure 11: Comparison of test results and IIW recommendation at S700

5.2. Effective notch stress approach

Using the stress concentration factor from chapter 4.3 multiplied with the results from the nominal stress approach, the results for the local stress approach are shown in Figure 12 and Figure 13. The recommended S/N-curve for as-welded condition (Hobbacher, 2016) is defined with  $m_I = 3$  and FAT 225, independently from the grade of steel. Applying the notch stress approach for S355 with HFMI-treated cruciform joints (Marquis and Barsoum, 2016) leads to FAT 320 and  $m_I = 5$ . Similarly, to the nominal stress approach for S355, the recommended and evaluated S/N-curves (see Figure 12) intersect in the finite life region, but the bulk of the test data points is still assessed conservatively. The evaluated results of the HFMI-treated specimen are largely consistent with the recommended S/N-curve proving the applicability of the effective notch stress approach for the studied HFMI-treated joints.

As in chapter 5.1 depicted, the evaluated test results with the effective notch stress approach for the S700 as-welded specimen show again a slight divergence to the recommended S/N-curve too, but once more, almost all data points are still assessed conservatively. The results for the high strength steel S700 in HFMI-treated condition are nearly congruent with the recommended S/N-curve again revealing sound practicability of the HFMI guideline.

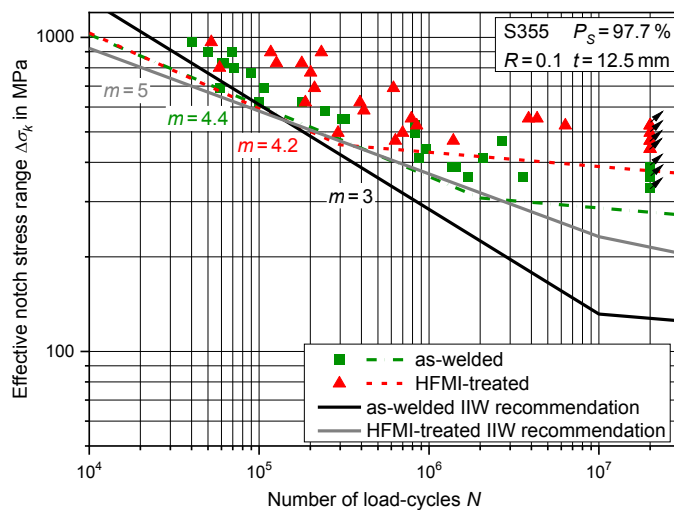


Figure 12: Results for S355 of effective notch stress fatigue test results and recommended S/N-curves

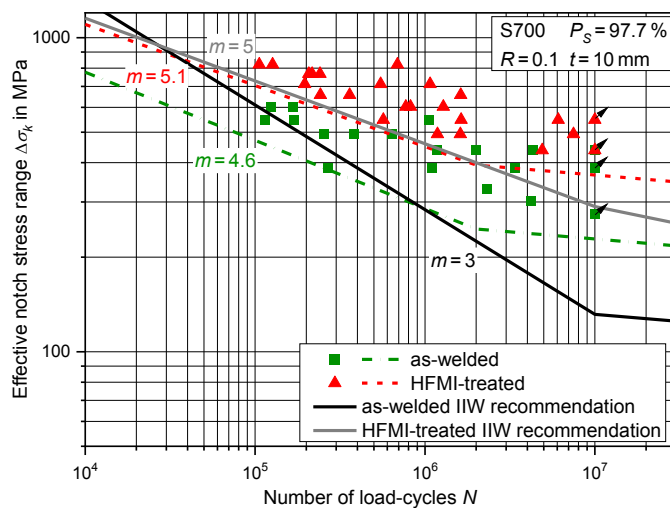


Figure 13 Results for S700 of effective notch stress fatigue test results and recommended S/N-curves

## 6. Conclusions

Based on the conducted work, focusing on the fatigue design of mild S355 and high-strength steel S700 cruciform joints in as-welded and HFMI-treated condition by both nominal and effective notch stress approach, the following scientific conclusions can be drawn:

- HFMI-treatment as post treatment method can significantly increase the fatigue performance of welded steel joints. Based on the investigated cruciform joints, a benefit factor in fatigue strength at two million load-cycles is evaluated as 1.35 for the mild steel S355, and as 1.59 for the high-strength steel S700.
- The fatigue design based on the nominal stress approach shows that both IIW recommendations are well applicable to assess the fatigue strength of as-welded and HFMI-treated cruciform joints in both steel grades. However, in case of the as-welded state, the design curves intersect with the statistically evaluated S/N-curves, which may be caused by enhanced specimen deformation. Nonetheless, the bulk of the test data points is still assessed conservatively.
- The fatigue design based on the effective notch stress approach also reveals a sound applicability of the local approach to assess the investigated test series. Again, the same trends occur in the as-welded state as observed using the nominal stress approach.

Besides experimental analyses, further focus is laid on the numerical investigation of the HFMI-treatment process in order to optimize HFMI process parameters in regard to local properties and further fatigue resistance (Ernould et al., 2019; Khurshid et al., 2017; Leitner et al., 2018c). Moreover, emphasizes should be given in the applicability of the HFMI-treatment to repair pre-fatigued structures, see also (Al-Karawi et al., 2021; Lefebvre et al., 2017; Leitner et al., 2016).

## References

- Al-Karawi, H., Bock und Polach, R.U.F. von, Al-Emrani, M., 2021. Fatigue life extension of existing welded structures via high frequency mechanical impact (HFMI) treatment. *Engineering Structures* 239, 112234.
- Baumgartner, J., Bruder, T., 2013. An efficient meshing approach for the calculation of notch stresses. *Welding in the World* 57, 137–145.
- Braun, M., Wang, X., 2021. A review of fatigue test data on weld toe grinding and weld profiling. *International Journal of Fatigue* 145, 106073.
- Dahle, T., 1998. Design fatigue strength of TIG-dressed welded joints in high-strength steels subjected to spectrum loading. *International Journal of Fatigue* 20, 677–681.
- Ernould, C., Schubnell, J., Farajian, M., Maciolek, A., Simunek, D., Leitner, M., Stoschka, M., 2019. Application of different simulation approaches to numerically optimize high-frequency mechanical impact (HFMI) post-treatment process. *Welding in the World* 63, 725–738.
- Friedrich, N., 2020. Experimental investigation on the influence of welding residual stresses on fatigue for two different weld geometries. *Fatigue & Fracture of Engineering Materials & Structures* 43, 2715–2730.
- Fu, Z., Ji, B., Kong, X., Chen, X., 2018. Effects of Hammer Peening on Fatigue Performance of Roof and U-Rib Welds in Orthotropic Steel Bridge Decks. *Journal of Materials in Civil Engineering* 30, 4018306.
- Fueki, R., Takahashi, K., Handa, M., 2019. Fatigue Limit Improvement and Rendering Defects Harmless by Needle Peening for High Tensile Steel Welded Joint. *Metals* 9, 143.
- Gan, J., Di Sun, Wang, Z., Luo, P., Wu, W., 2016. The effect of shot peening on fatigue life of Q345D T-welded joint. *Journal of Constructional Steel Research* 126, 74–82.
- Haagensen, P.J., Maddox, S.J. IIW recommendations on methods for improving the fatigue strength of welded joints. IIW-2142-10. WP Woodhead Publishing, Oxford, Cambridge, Philadelphia, New Delhi.
- Hansen, A.V., Agerskov, H., Bjørnbak-Hansen, J., 2007. Improvement of Fatigue Life of Welded Structural

- Components by Grinding. *Welding in the World* 51, 61–67.
- Harati, E., Karlsson, L., Svensson, L.-E., Dalaei, K., 2015. The relative effects of residual stresses and weld toe geometry on fatigue life of weldments. *International Journal of Fatigue* 77, 160–165.
- Harati, E., Svensson, L.-E., Karlsson, L., Widmark, M., 2016. Effect of high frequency mechanical impact treatment on fatigue strength of welded 1300 MPa yield strength steel. *International Journal of Fatigue* 92, 96–106.
- Hensel, J., Eslami, H., Nitschke-Pagel, T., Dilger, K., 2019. Fatigue Strength Enhancement of Butt Welds by Means of Shot Peening and Clean Blasting. *Metals* 9, 744.
- Hirohata, M., 2017. Effect of post weld heat treatment on steel plate deck with trough rib by portable heat source. *Welding in the World* 61, 1225–1235.
- Hobbacher, A.F., 2016. *Recommendations for Fatigue Design of Welded Joints and Components*. Springer International Publishing, Cham.
- Huo, L., Wang, D., Zhang, Y., 2005. Investigation of the fatigue behaviour of the welded joints treated by TIG dressing and ultrasonic peening under variable-amplitude load. *International Journal of Fatigue* 27, 95–101.
- Khurshid, M., Leitner, M., Barsoum, Z., Schneider, C., 2017. Residual stress state induced by high frequency mechanical impact treatment in different steel grades – Numerical and experimental study. *International Journal of Mechanical Sciences* 123, 34–42.
- Kinoshita, K., Banno, Y., Ono, Y., Yamada, S., Handa, M., 2019. Fatigue Strength Improvement of Welded Joints of Existing Steel Bridges by Shot-Peening. *International Journal of Steel Structures* 19, 495–503.
- Lefebvre, F., Peyrac, C., Elbel, G., Revilla-Gomez, C., Verdu, C., Buffière, J.-Y., 2017. HFMI: understanding the mechanisms for fatigue life improvement and repair of welded structures. *Welding in the World* 61, 789–799.
- Leitner, M., 2017. Influence of effective stress ratio on the fatigue strength of welded and HFMI-treated high-strength steel joints. *International Journal of Fatigue* 102, 158–170.
- Leitner, M., Barsoum, Z., 2020. Effect of increased yield strength, R-ratio, and plate thickness on the fatigue resistance of high-frequency mechanical impact (HFMI)-treated steel joints. *Welding in the World* 64, 1245–1259.
- Leitner, M., Barsoum, Z., Schäfers, F., 2016. Crack propagation analysis and rehabilitation by HFMI of pre-fatigued welded structures. *Welding in the World* 60, 581–592.
- Leitner, M., Khurshid, M., Barsoum, Z., 2017a. Stability of high frequency mechanical impact (HFMI) post-treatment induced residual stress states under cyclic loading of welded steel joints. *Engineering Structures* 143, 589–602.
- Leitner, M., Mössler, W., Putz, A., Stoschka, M., 2015. Effect of post-weld heat treatment on the fatigue strength of HFMI-treated mild steel joints. *Welding in the World* 59, 861–873.
- Leitner, M., Murakami, Y., Farajian, M., Remes, H., Stoschka, M., 2018a. Fatigue Strength Assessment of Welded Mild Steel Joints Containing Bulk Imperfections. *Metals* 8, 306.
- Leitner, M., Ottersböck, M., Pußwald, S., Remes, H., 2018b. Fatigue strength of welded and high frequency mechanical impact (HFMI) post-treated steel joints under constant and variable amplitude loading. *Engineering Structures* 163, 215–223.
- Leitner, M., Pauer, P., Kainzinger, P., Eichlseder, W., 2017b. Numerical effects on notch fatigue strength assessment of non-welded and welded components. *Computers & Structures* 191, 51–61.
- Leitner, M., Simunek, D., Shah, S.F., Stoschka, M., 2018c. Numerical fatigue assessment of welded and HFMI-treated joints by notch stress/strain and fracture mechanical approaches. *Advances in Engineering Software* 120, 96–106.
- Leitner, M., Stoschka, M., 2020. Effect of load stress ratio on nominal and effective notch fatigue strength assessment of HFMI-treated high-strength steel cover plates. *International Journal of Fatigue* 139, 105784.
- Leitner, M., Stoschka, M., Barsoum, Z., Farajian, M., 2020. Validation of the fatigue strength assessment of HFMI-treated steel joints under variable amplitude loading. *Welding in the World* 64, 1681–1689.
- Leitner, M., Stoschka, M., Eichlseder, W., 2014. Fatigue enhancement of thin-walled, high-strength steel joints by high-frequency mechanical impact treatment. *Welding in the World* 58, 29–39.
- Leitner, M., Stoschka, M., Ottersböck, M., 2017c. Fatigue assessment of welded and high frequency mechanical impact (HFMI) treated joints by master notch stress approach. *International Journal of Fatigue* 101, 232–243.
- Liinalampi, S., Remes, H., Romanoff, J., 2019. Influence of three-dimensional weld undercut geometry on fatigue-effective stress. *Welding in the World* 63, 277–291.
- Marquis, G.B., Barsoum, Z., 2016. IIW Recommendations for the HFMI Treatment. For Improving the Fatigue

- Strength of Welded Joints. Springer Singapore, Singapore, s.l.
- Mettänen, H., Nykänen, T., Skriko, T., Ahola, A., Björk, T., 2020. Fatigue strength assessment of TIG-dressed ultra-high-strength steel fillet weld joints using the 4R method. *International Journal of Fatigue* 139, 105745.
- Nitschke-Pagel, T., Hensel, J., 2021. An enhancement of the current design concepts for the improved consideration of residual stresses in fatigue-loaded welds. *Welding in the World* 65, 643–651.
- Ottersböck, M., Leitner, M., Stoschka, M., 2018. Impact of Angular Distortion on the Fatigue Performance of High-Strength Steel T-Joints in as-Welded and High Frequency Mechanical Impact-Treated Condition. *Metals* 8, 302.
- Ottersböck, M.J., Leitner, M., Stoschka, M., 2021. Characterisation of actual weld geometry and stress concentration of butt welds exhibiting local undercuts. *Engineering Structures* 240, 112266.
- Ottersböck, M.J., Leitner, M., Stoschka, M., Maurer, W., 2019. Analysis of fatigue notch effect due to axial misalignment for ultra high-strength steel butt joints. *Welding in the World* 63, 851–865.
- RAVI, S., BALASUBRAMANIAN, V., NEMATNASSER, S., 2005. Influences of post weld heat treatment on fatigue life prediction of strength mis-matched HSLA steel welds. *International Journal of Fatigue* 27, 547–553.
- Schubnell, J., Hardenacke, V., Farajian, M., 2017. Strain-based critical plane approach to predict the fatigue life of high frequency mechanical impact (HFMI)-treated welded joints depending on the material condition. *Welding in the World* 61, 1199–1210.
- Sonsino, C.M., 2009a. A Consideration of Allowable Equivalent Stresses for Fatigue Design of Welded Joints According to the Notch Stress Concept with the Reference Radii  $r_{ref} = 1.00$  and  $0.05$  mm. *Welding in the World* 53, R64-R75.
- Sonsino, C.M., 2009b. Effect of residual stresses on the fatigue behaviour of welded joints depending on loading conditions and weld geometry. *International Journal of Fatigue* 31, 88–101.
- Tai, M., Miki, C., 2014. Fatigue strength improvement by hammer peening treatment—verification from plastic deformation, residual stress, and fatigue crack propagation rate. *Welding in the World* 58, 307–318.
- Trudel, A., Lévesque, M., Brochu, M., 2014. Microstructural effects on the fatigue crack growth resistance of a stainless steel CA6NM weld. *Engineering Fracture Mechanics* 115, 60–72.
- Tsay, L.W., Tsay, C.Y. The effect of microstructures on the fatigue crack growth in Ti-6Al-4V laser welds.
- Yamaguchi, N., Lemoine, G., Shiozaki, T., Tamai, Y., 2019. Effect of microstructures on notch fatigue properties in ultra-high strength steel sheet welded joint. *International Journal of Fatigue* 129, 105233.
- Yildirim, H.C., Marquis, G.B., 2012a. Fatigue strength improvement factors for high strength steel welded joints treated by high frequency mechanical impact. *International Journal of Fatigue* 44, 168–176.
- Yildirim, H.C., Marquis, G.B., 2012b. Overview of Fatigue Data for High Frequency Mechanical Impact Treated Welded Joints. *Welding in the World* 56, 82–96.
- Yildirim, H.C., Marquis, G.B., 2014. Notch stress analyses of high-frequency mechanical impact-improved welds by using  $\rho_f = 1$  mm and  $\rho_f = \rho + 1$  mm approaches. *Fatigue & Fracture of Engineering Materials & Structures* 37, 561–569.
- Yildirim, H.C., Marquis, G.B., Barsoum, Z., 2013. Fatigue assessment of high frequency mechanical impact (HFMI)-improved fillet welds by local approaches. *International Journal of Fatigue* 52, 57–67.
- Yıldırım, H.C., Leitner, M., Marquis, G.B., Stoschka, M., Barsoum, Z., 2016. Application studies for fatigue strength improvement of welded structures by high-frequency mechanical impact (HFMI) treatment. *Engineering Structures* 106, 422–435.
- Zhang, Y.-H., Maddox, S.J., 2009. Fatigue life prediction for toe ground welded joints. *International Journal of Fatigue* 31, 1124–1136.